

Comparative incapacitation study between aluminium-steel and all-steel witness packs used to record behind-armour debris from a shaped charge impact

Yves Baillargeon, M. Eng.
Patrick Lacoursière, jr. Eng.
Alexandra Sirois, M. Eng.
Weapons Effects and Protection Section
DRDC – Valcartier Research Centre

Defence Research and Development Canada

Scientific Report
DRDC-RDDC-2014-R147
December 2014

Template in use: SR Advanced_Oct_Release_EN_2015-07-17.dot

- © Her Majesty the Queen in Right of Canada, as represented by the Minister of National Defence, 2014
- © Sa Majesté la Reine (en droit du Canada), telle que représentée par le ministre de la Défense nationale, 2014

Abstract

Two witness pack configurations are widely used by The Technical Cooperation Program (TTCP) members to record behind armour debris: the all-steel pack and an aluminium-steel pack. Ballistic impacts were performed for a given shaped charge threat against a specific target to analyse the difference in the behind-armour debris measured using the two different witness packs. This report showed a higher number of fragments recorded and a higher level of incapacitation measured using the aluminium-steel witness pack. The first witness pack layers of the aluminium-steel witness pack are more easily perforated by fragments since they are made of 1 mm of aluminium compared to 0.8 mm of steel for the all-steel pack. Based on this report, it is recommended continuing using the aluminium-steel witness pack for behind-armour debris measurement of a shaped charge impact on a metallic target.

Significance to defence and security

The all-steel witness pack used in this report offers the advantage of being low cost and more resistant than the aluminium-steel witness pack (i.e., less bending, smaller hole in the middle of the witness pack from shaped charge jet penetration and hole diameters in the witness plate closer to the real size of the fragment). However, based on this study, the first witness plate of the all-steel witness pack is too robust and not all behind armour debris are recorded. This can lead to underestimation of the incapacitation level of the crews after impact. Therefore, for that type of threat, which produces a lot of relatively low perforation capability fragments, the aluminium-steel witness pack is more suitable.

Résumé

Deux panneaux témoins sont grandement utilisés par les membres du programme de coopération technique (TTCP) pour consigner les débris derrière le blindage : le panneau tout acier et celui en acier à l'aluminium. Des tests d'impact balistique ont été réalisés avec une charge creuse donnée sur une cible déterminée pour analyser la différence de mesure des débris derrière le blindage à l'aide des deux panneaux témoins. Les résultats du présent rapport démontrent qu'un plus grand nombre de fragments a été constaté et qu'un niveau plus élevé d'incapacité a été mesuré à l'aide du panneau témoin en acier à l'aluminium. Les premières couches du panneau témoin en acier à l'aluminium sont plus facilement perforées par les fragments, car elles sont constituées de 1 mm d'aluminium comparativement à 0,8 mm dans le cas du panneau tout acier. En se basant sur le présent rapport, on recommande de continuer à utiliser le panneau témoin en acier à l'aluminium pour mesurer les débris derrière le blindage à la suite de l'impact d'une charge creuse sur une cible métallique.

Importance pour la défense et la sécurité

Le panneau témoin tout acier utilisé dans le présent rapport a l'avantage d'être peu coûteux et plus résistant que celui en acier à l'aluminium (c.-à-d. moins de déformation, trous de plus petite taille au milieu du panneau témoin causés par la perforation à charge creuse, et trous dans la plaque témoin dont le diamètre est plus près de la taille réelle du fragment). Cependant, en se basant sur la présente étude, la première plaque du panneau témoin tout acier est trop robuste, et les débris derrière le blindage ne sont pas tous consignés. Cela peut amener à sous-estimer le niveau d'incapacité des équipages après impact. Donc, pour ce type de menace qui produit beaucoup de fragments à capacité de perforation relativement faible, le panneau témoin en acier à l'aluminium est plus adéquat.

Table of contents

Abstract	i
Significance to defence and security	i
Résumé	ii
Importance pour la défense et la sécurité	ii
Table of contents	iii
List of figures	iv
List of tables	v
1 Introduction	1
2 Test material	2
2.1 Aluminum-steel WP	2
2.2 All-steel WP	2
2.3 Ammunition	2
2.4 Target	2
3 Test set up	3
4 Test results	4
4.1 Fragments recorded	4
4.2 Fragment distribution	5
4.2.1 Fragment mass and velocity calculation	5
4.2.2 Fragment mass distribution	7
4.2.3 Fragment velocity distribution	10
4.3 PI comparison	13
4.3.1 PI calculation	13
4.3.2 PI results	14
5 Conclusion	16
List of symbols/abbreviations/acronyms/initialisms	17

List of figures

Figure 1:	Alu-St WP.	2
Figure 2:	Test set up.	3
Figure 3:	Fragment speed versus mass of each plate from Alu-St WP and All-St WP.. . . .	5
Figure 4:	THOR velocity calculation algorithm in DeCaM.	6
Figure 5:	Fragment mass distribution.	7
Figure 6:	Fragments ranging from 0 to 0, 25 g.	8
Figure 7:	Fragment masses according to their position for three shots (Alu-St WP).	9
Figure 8:	Fragment masses according to their position for four shots (All-St WP).	9
Figure 9:	Fragment velocities according to their position for three shots (Alu-St WP).	10
Figure 10:	Fragment velocities according to their position for four shots (All-St WP).	11
Figure 11:	BAD cloud for velocity measurements.	12
Figure 12:	Fragment velocity distribution..	13
Figure 13:	PID related to the cone angle based on Kokinakis.	14
Figure 14:	PIA related to the cone angle based on Kokinakis.	15

List of tables

Table 1:	Average number of fragments that were stopped after each plate.	4
Table 2:	Fragment velocities measured on high speed video.	12

This page intentionally left blank.

1 Introduction

The goal of this paper is to compare the sensitivity of two different metallic Witness Packs (WP) designed to record Behind-Armour Debris (BAD) resulting from a shaped charge jet impact on a steel target. The main difference between the two WP is the material type (i.e., aluminium or steel) and layer thicknesses. Three shots were fired for each WP configuration. Each WP was analysed to extract the position, mass, velocity and lethality using the Debris Characterisation and Modelling software (Debris Characterisation and Modelling software (DeCaM) developed by BMT Fleet Technology with Defence Research and Development Canada (DRDC) contracts), THOR¹ penetration equations and Kokinakis incapacitation prediction model. Each WP will be first described, the test set up presented and finally, the results will give a comparison of the number of fragments, the mass and velocity distribution and the Percentage of Incapacitation (PI).

¹ Ballistic Analysis Laboratory. “The resistance of Various Metallic Materials to Perforation by Steel fragments: Empirical Relationships for fragment residual velocity and Weigth (U)”, Project THOR, technical report 47 (Apr. 1961) Confidential.

2 Test material

In this chapter, both WPs are presented and compared. These differences lead to a different threshold fragment energy required to be recorded by the WP.

2.1 Aluminum-steel WP

The aluminium-steel (Alu-St) WP is made of four plates (see Figure 1). Each plate is spaced by 25 mm of polystyrene foam (15 kg/m^3). The first and second plates are made of 1 mm of aluminium-1100 H14. The third plate is also made with aluminium-1100 H14 but has a thickness of 3 mm. The last plate is made of steel-1010/1020 with a thickness of 1.5 mm.



Figure 1: Alu-St WP.

2.2 All-steel WP

The all-steel (All-St) WP consists of five layers of steel-1010/1020 with the following thicknesses: 0.8 mm, 0.8 mm, 1.6 mm, 1.6 mm and 3.2 mm. All layers are separated by a 25 mm polystyrene foam sheet.

2.3 Ammunition

The Shaped Charge (SC) used was the same for all tests and had a copper cone liner.

2.4 Target

Targets were 25 mm thick Rolled Homogenous Armour (RHA) steel plates for all tests.

3 Test set up

Three SC impacts were performed to record debris with each WP type. The shaped charges were fired at Build in Standoff (BISO) and maintained in a vertical plane with the help of a polystyrene bloc. The frontal surface of the WPs were always positioned at 600 mm from the back face of the target (see Figure 2). After each test, each WP was scanned and analysed using the semi-automatic Witness Pack Analysis System (WPAS developed by Imago Video Trackers with DRDC contracts). With the WPAS, the position and area of each hole resulting from a fragment impact is found and the data is then analysed with DeCaM which gives an estimate of the mass and velocity of each fragment using a penetration model.

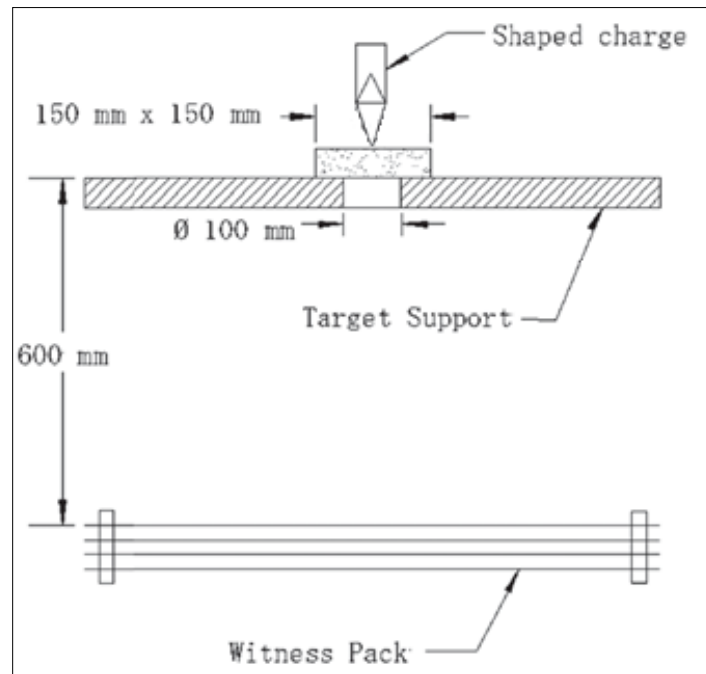


Figure 2: Test set up.

A high speed camera was used to film the behind armour debris cloud and measure selected fragment velocities.

4 Test results

The results distribution results for both the Alu-St WP and All-St WP are presented in this section. The percentage of incapacitation is presented for comparison of both materials from an occupant's safety point of view.

4.1 Fragments recorded

Each plate was scanned to check how many fragments hit the different plates of the WP. Table 1 gives the average number of fragments that were stopped after each plate for each WP type. The numbers of fragments are averaged from three identical shots for each WP type. The aluminium plates registered significantly more fragments than their steel counterparts.

Table 1: Average number of fragments that were stopped after each plate.

Plate #	All-St WP	Alu-St WP	Difference (Alu-St vs All-St WP)
1	480	701	+221
2	32	286	+254
3	4	9	+5
4	3	1	-2
5	1	N/A	N/A
Total:	520	997	+477

The difference in the number of fragments recorded for the second plate of the Alu-St WP and the first plate of the All-St WP should not be that different, because the velocity required for a fragment to perforate the two first 1 mm aluminium sheets of the Alu-St WP should be similar to the velocity required to perforate the first layer made of 0.8 mm of steel from the All-St WP (see Figure 3 produced using THOR Equation (2) while neglecting the polystyrene foam). The large difference in the number of fragments recorded (i.e., 480 vs 286) can be explained by the fact that this extra polystyrene foam sheet between the two aluminum sheets requires a minimum level of energy to be perforated. Further studies should be performed to assess the amount of energy that the polystyrene foam removed from the low energy fragments.

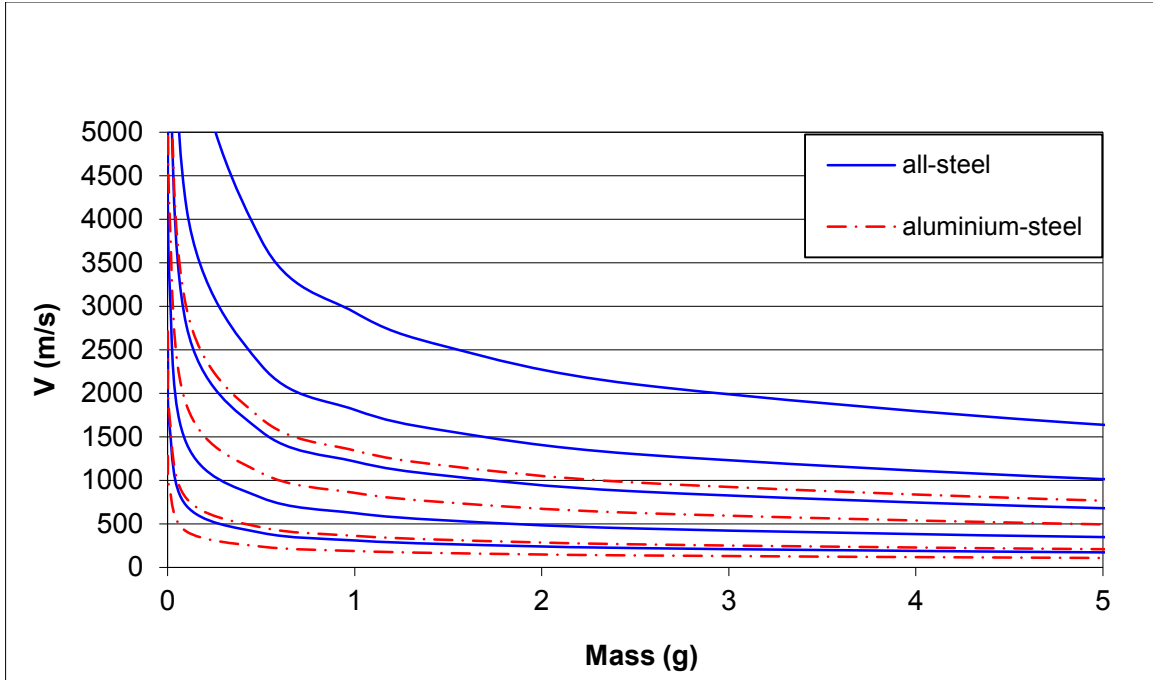


Figure 3: Fragment speed versus mass of each plate from Alu-St WP and All-St WP.

4.2 Fragment distribution

4.2.1 Fragment mass and velocity calculation

Each fragment mass is considered constant throughout penetration of the plates of the witness pack. The fragment mass m_s is calculated using:

$$m_s = \left(\frac{A_{plate1}}{K} \right)^{3/2}. \quad (1)$$

A_{plate1} is the area of the hole created in the first plate from the WP and K is the fragment shape factor.

The fragment's velocities were calculated using the THOR penetration Equations (2) (3) implemented in the DeCaM software. Two THOR equations were used in the algorithm developed for DeCaM as shown in Figure 4.

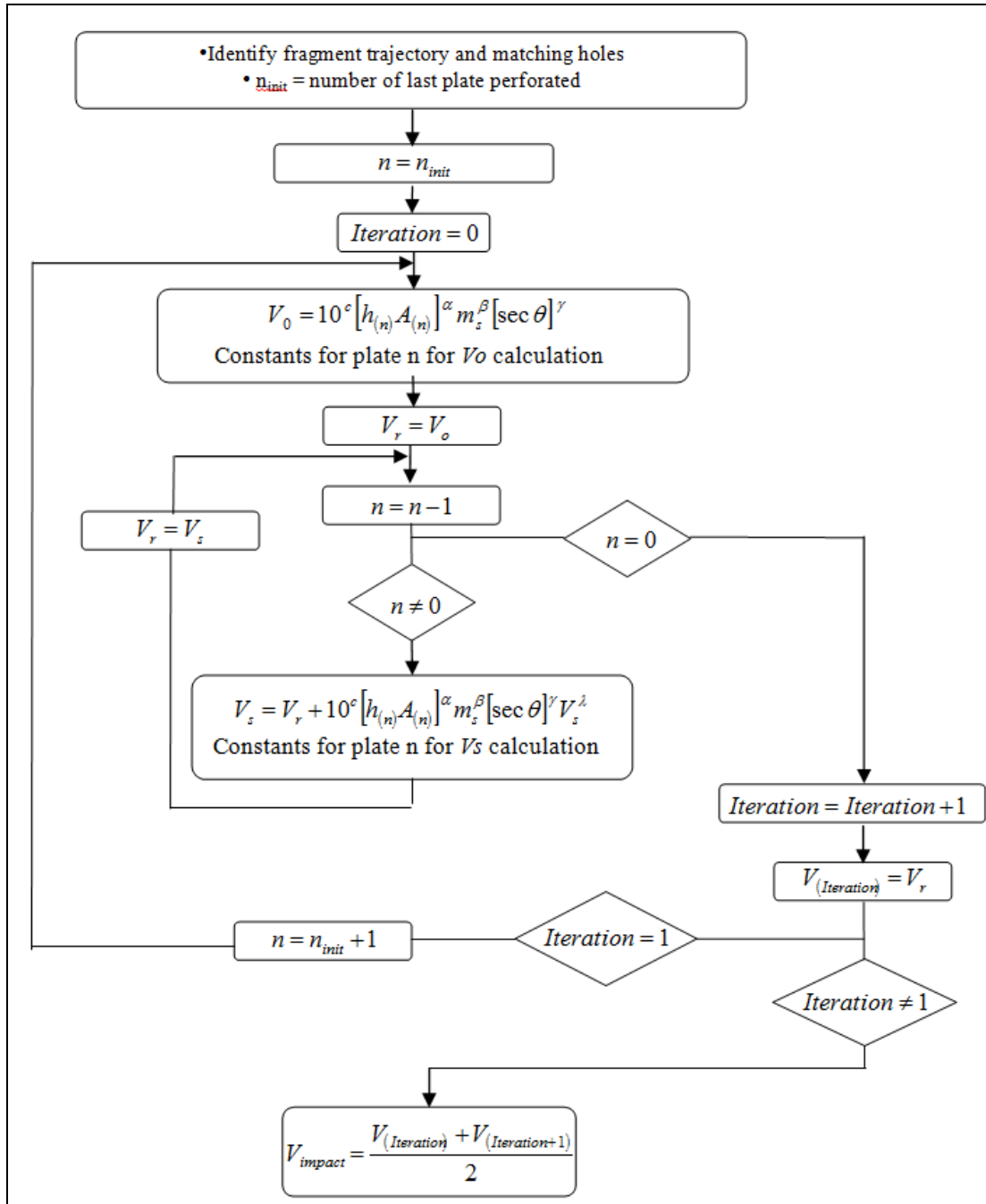


Figure 4: THOR velocity calculation algorithm in DeCaM.

The first equation calculates the residual velocity V_s (ft/s) and the second calculates the velocity for a fragment or projectile to just penetrate a plate of a certain thickness:

$$V_r = V_s - 10^c (hA)^\alpha m_s^{\beta 1} (\sec \omega)^\gamma V_s^\lambda, \quad (2)$$

$$V_0 = 10^{c1} (hA)^{\alpha 1} m_s^{\beta 1} (\sec \omega)^{\lambda 1}. \quad (3)$$

Where m_s is the projectile initial mass (grain), h the target thickness (inch), A is the area of the hole (inch²), ω is the angle of the shot with respect to normal of the target and $c, \alpha, \beta, \gamma, \lambda$ are constants related to the target material.

4.2.2 Fragment mass distribution

Figure 5 shows the fragment mass distribution for both witness packs. Figure 6 shows the same fragment mass distribution focussing on masses lighter than 0.25 g. The majority of the extra fragments registered by the Alu-St WP had a very small mass and therefore not enough energy to perforate the 0.8 mm steel plate (first layer of the All-St WP).

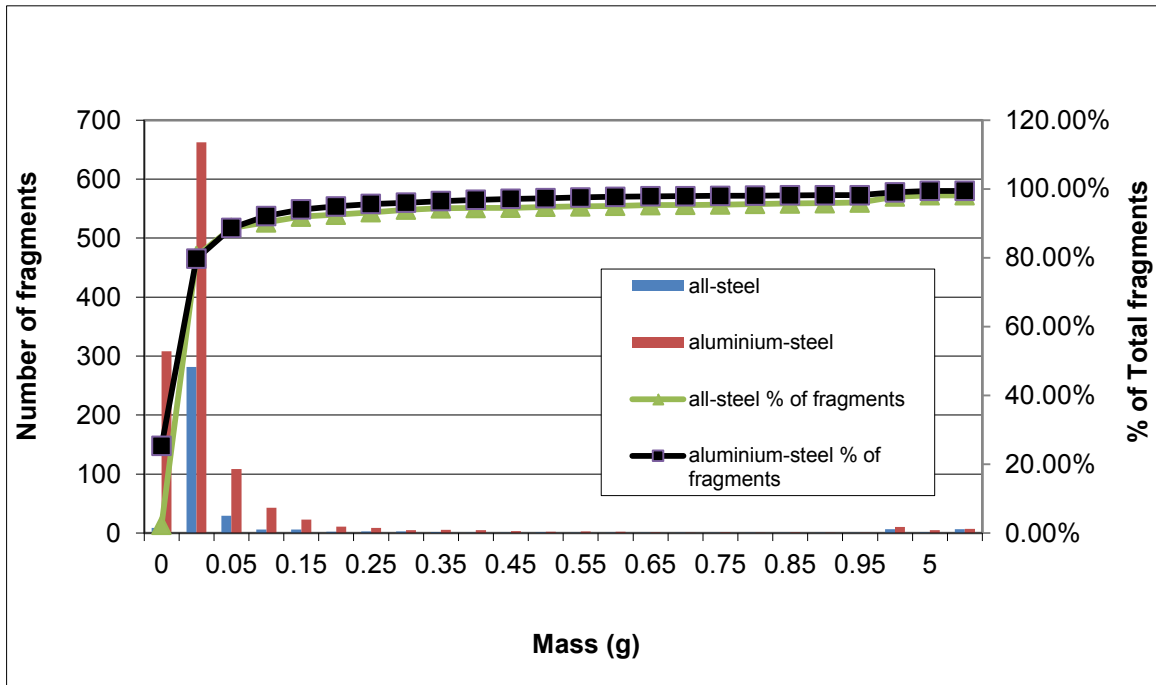


Figure 5: Fragment mass distribution.

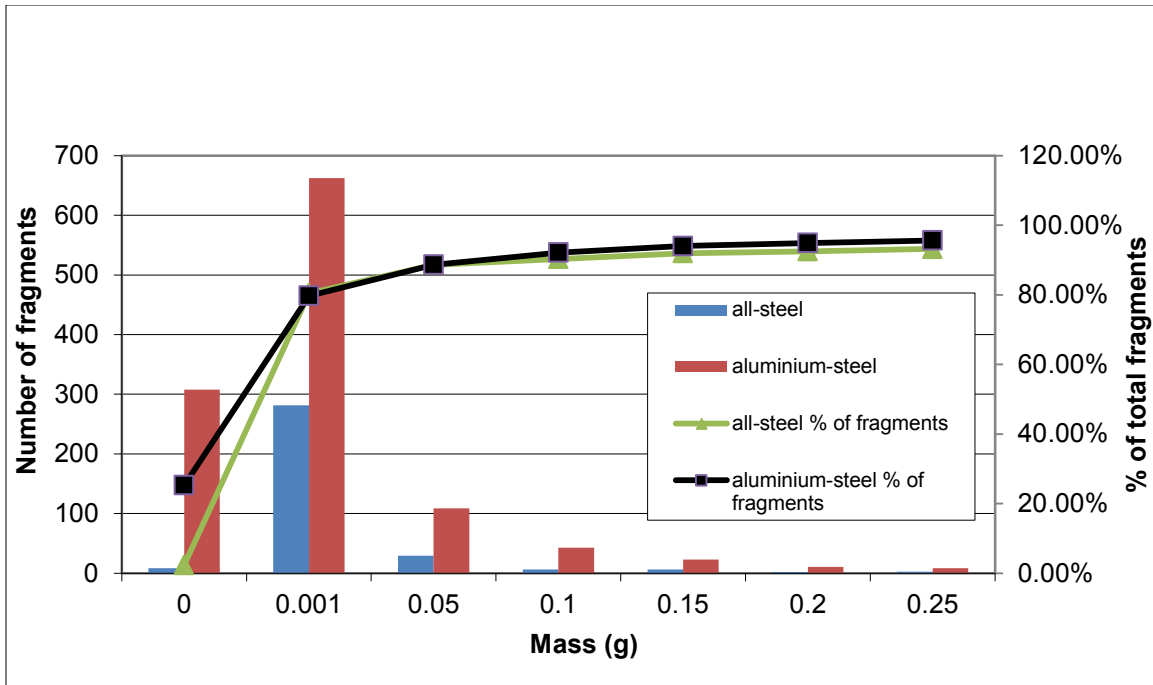


Figure 6: Fragments ranging from 0 to 0, 25 g.

As seen in Figure 6, the bulk of the fragments are from zero to 0,001 g. In the Alu-St WP, that range of mass represents a quarter of the total number fragments collected.

Figure 7 and 8 show the fragment masses with respect to positions for the three shots for each WP configuration. A larger number of heavier fragments are observed for the All-St WP. Firing a larger number of rounds would probably lead to a more precise statistical mass distribution especially for a range of mass with a limited population.

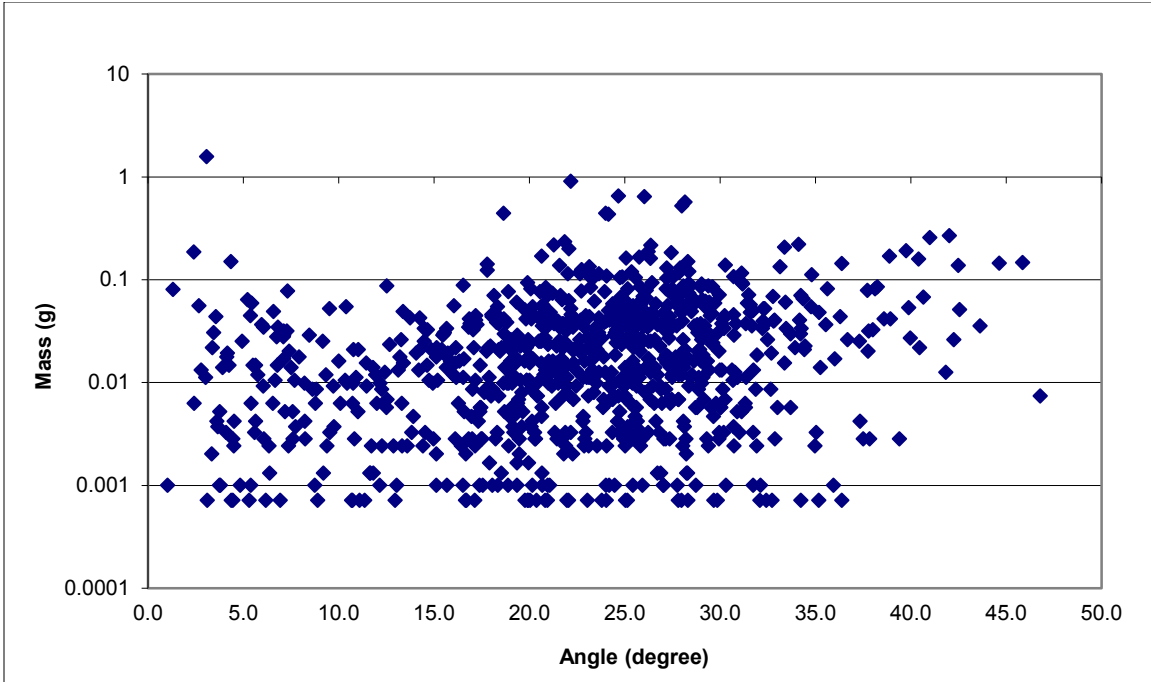


Figure 7: Fragment masses according to their position for three shots (Alu-St WP).

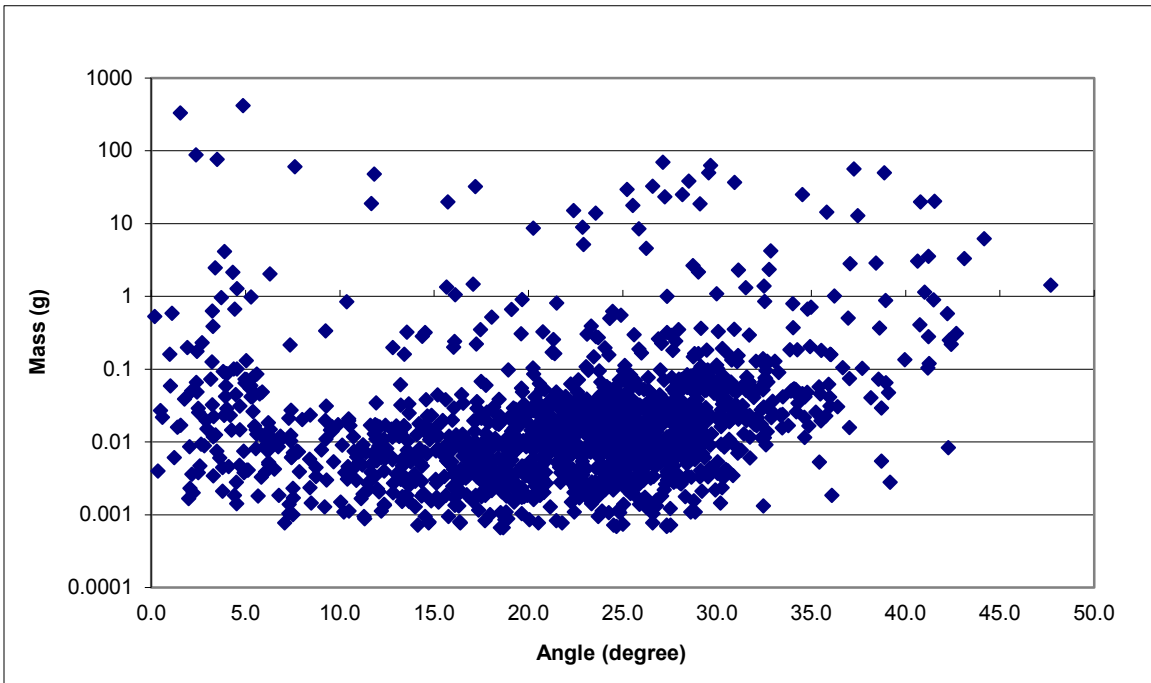


Figure 8: Fragment masses according to their position for four shots (All-St WP).

4.2.3 Fragment velocity distribution

Figure 9 and 10 show the fragment velocities with respect to position for the three shots for each WP configuration. The Alu-St WP show less scattering in the values obtained, especially at higher velocities.

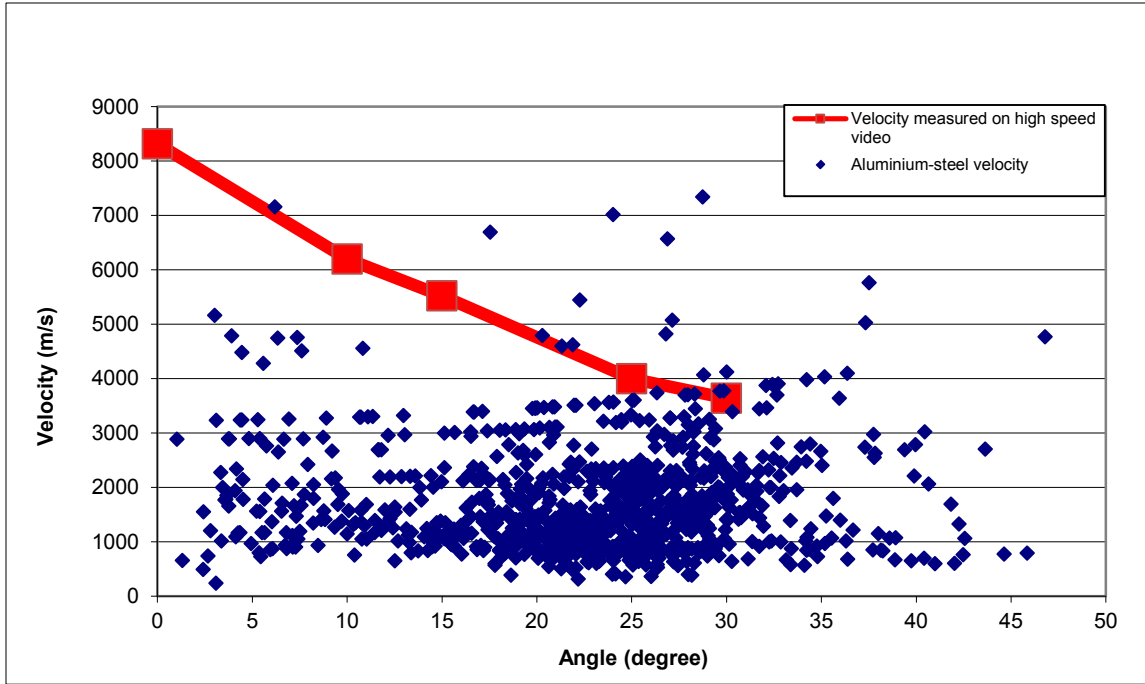


Figure 9: Fragment velocities according to their position for three shots (Alu-St WP).

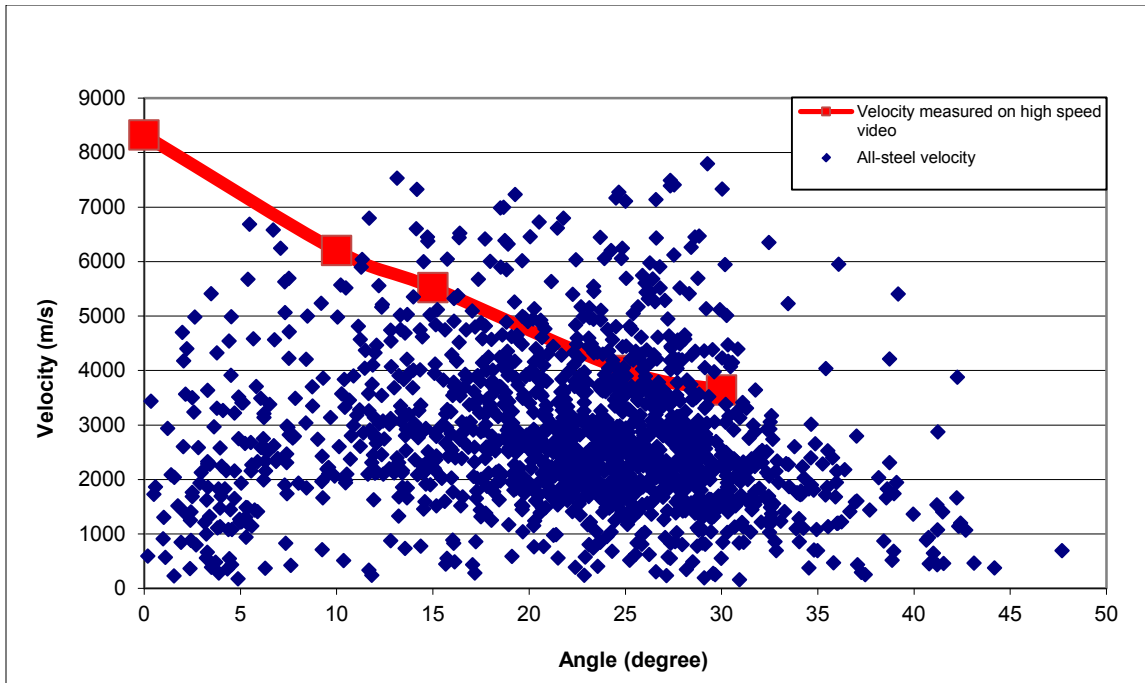


Figure 10: Fragment velocities according to their position for four shots (All-St WP).

Figure 11 shows two images from a high speed video camera used to record the faster behind armour debris at different angles after one of the six behind-armour debris tests. Table 2 shows the actual measured velocities. Those values are included in Figures 9 and 10. The velocity values above the measured velocities on high speed video camera are a potential source of error coming from the DeCam software (i.e., overestimated velocities). The All-St WP has more fragments with velocities higher than the velocities measured on high speed camera. This indicates that an analysis done using All-St WPs might overestimate fragment velocities more than an analysis done using Alu-St WPs. More tests are required to determine if this is the case. Figure 12 shows the fragment velocity count for both WP configurations. More low velocity fragments were recorded with the aluminum-steel packs.

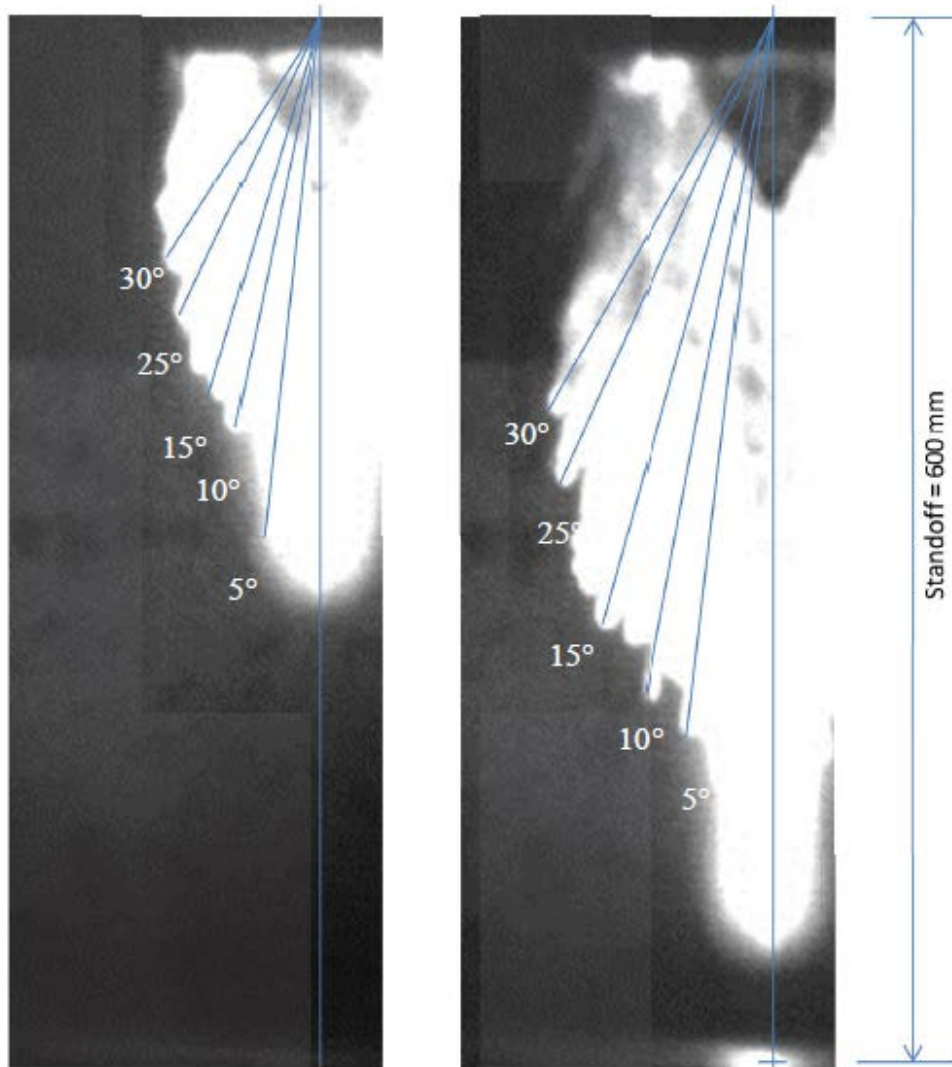


Figure 11: BAD cloud for velocity measurements.

Table 2: Fragment velocities measured on high speed video.

Azimuth angle (°)	Velocity measured on High speed video (HSV) (m/s)
0 (jet tip)	8320
10	6200
15	5520
25	4000
30	3640

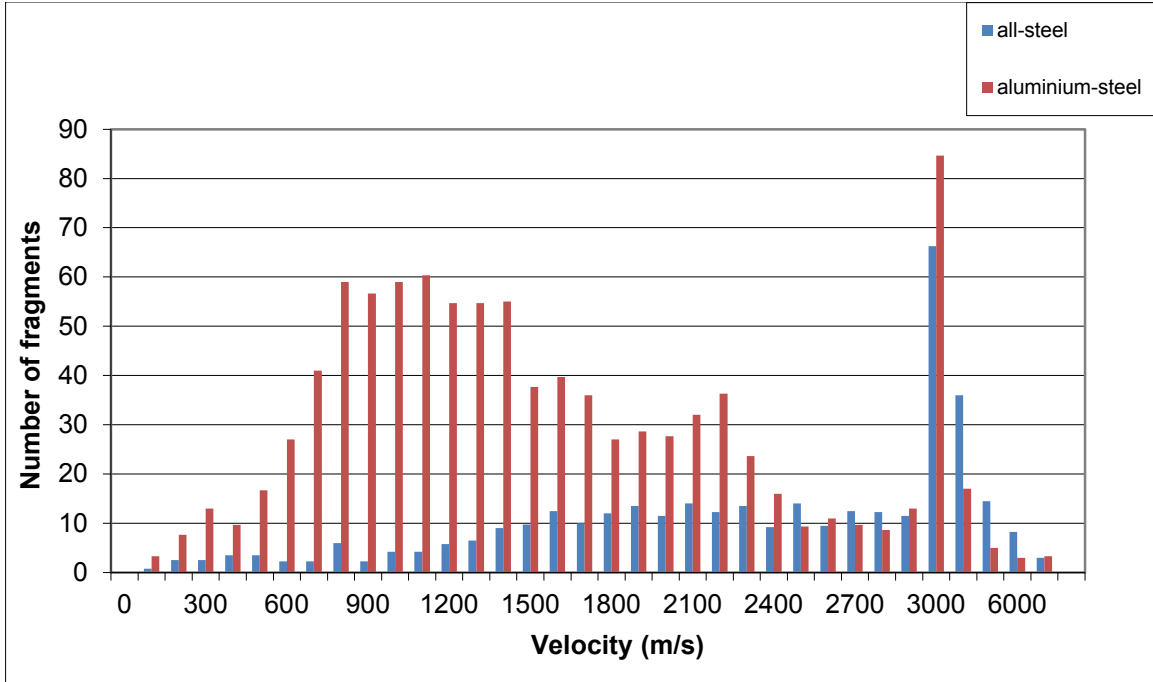


Figure 12: Fragment velocity distribution.

4.3 PI comparison

4.3.1 PI calculation

The PI is calculated by the amount of debris (fragments) that an occupant will receive depending on his position related to the debris cloud centroid. The occupants are assumed to be sitting at 60 cm standoff from the wall impacted by the SC.

The PI is calculated with lateral offsets ranging from 72 cm (50° offset angle) where the subject is completely out of range from the debris cone to 0 cm where the subject is hit by half the debris cone. Equation (4) shows that the PI represents the cumulative effect of all fragments impacting the occupant:

$$PI = 1 - \prod_{i=1}^n (1 - \lambda_i). \quad (4)$$

Where λ_i is the weighted expected level of incapacitation induced by fragment i , for fragments ranging from one to n fragments impacting the occupant, λ_i is calculated by:

$$\lambda_i = PI_i * PHit_i. \quad (5)$$

Where PI_i depends on the fragment mass m (grain) and velocity (ft/s) and $PHit_i$ is the probability of a fragment to impact the exposed surface area:

$$PI_i = e^{-a(mv^{3/2}-b)^n}, \quad (6)$$

$$PHit_i = \frac{S}{C} = \cos^{-1} \left(\frac{\tan \theta_1}{\tan \theta_2} \right) / \pi. \quad (7)$$

Parameters a, b and n depend on the PI criterion used. In the analysis presented here the Percentage of Incapacitation Defence-30 sec (PID) and Percentage of Incapacitation Attack-5 min (PIA) were used. θ_1 is the angle between the centre of the WP and the edge of the area covered. θ_2 is the angle between the centre of the WP and the fragment location. S is the length of an arc from the circle and C is the circumference of the circle made with the distance between the centre of the WP and the fragment.

4.3.2 PI results

Figure 13 shows that the PID 30 sec starts decreasing more steeply with the All-St WP PID than the Alu-St WP PID. However, at 30° a large decrease in PID starts occurring for both WP configurations. A difference of about 15% in PID and PIA is reported between the Alu-St WP and the All-St WP at 35°. This leads us to believe that Alu-St WP is more representative of the incapacitation from BAD.

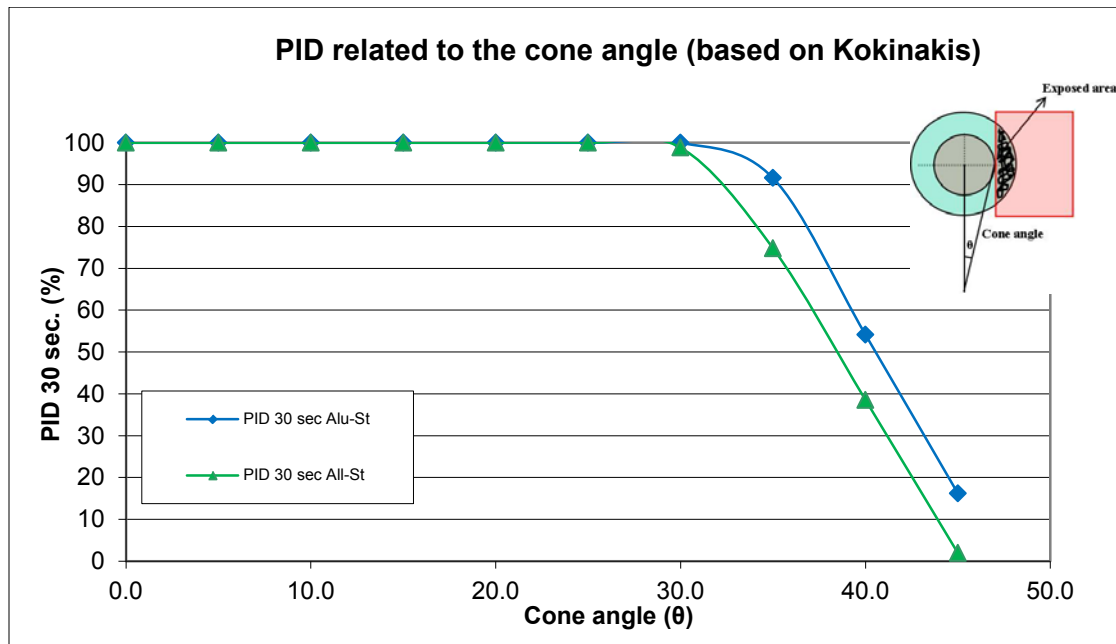


Figure 13: PID related to the cone angle based on Kokinakis.

Figure 14 shows the PIA from both experiments and the trend is similar. The same conclusions can be drawn as for the PID 30 sec.

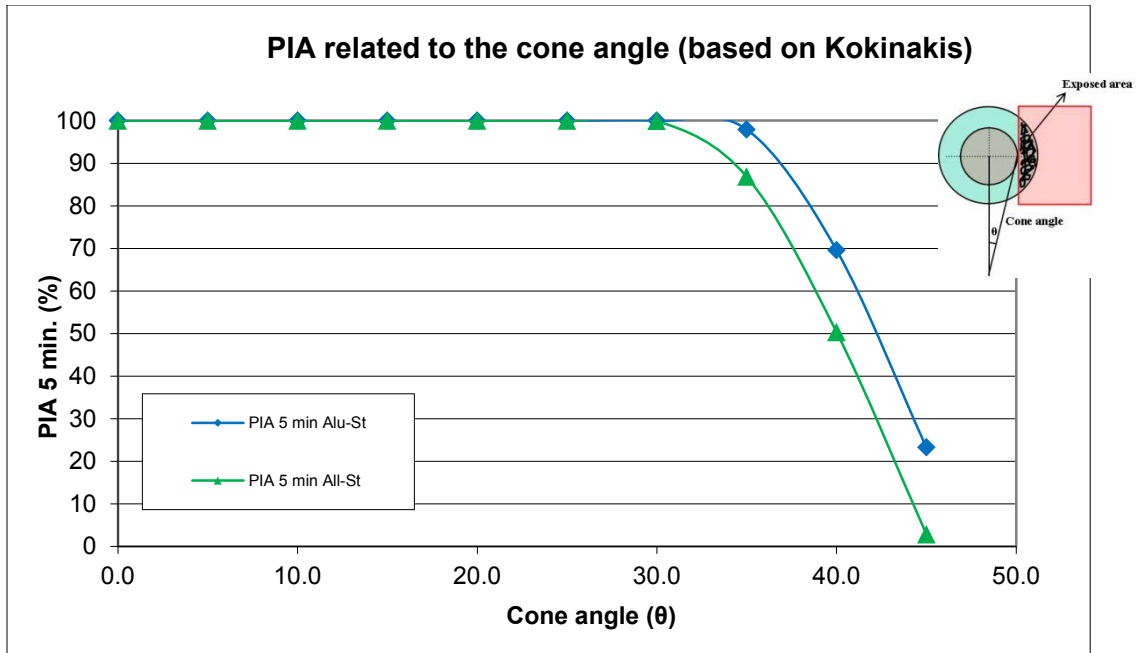


Figure 14: PIA related to the cone angle based on Kokinakis.

5 Conclusion

Six shaped charges were fired with two different types of WPs (Alu-St and All-St). The goal was to compare debris cloud characteristics extracted from the two types of WPs. The THOR empirical penetration model algorithm implemented in the DeCaM software was used to calculate the mass and velocity of each fragment registered in the WPs. From this data the PID and PIA were calculated for each fragment in each WP. Fragment mass and velocity distributions were used to highlight the differences between the Alu-St WP and the All-St WP. A larger number of fragments were recorded with the Alu-St WP. The analysis of the Alu-St WP also shows generally lower residual fragment velocities than for the All-St WP. Adding to these findings, the larger number of fragments recorded on the first layer of the Alu-St WP shows that the 1mm aluminium sheet is capable of recording more fragments than the 0.8mm of steel. The Alu-St WP is more sensitive to the smaller, lower mass fragments. Although the capability to perforate the first layer of the All-St WP (0.8mm of steel) was expected to be similar to the capability to perforate the two first layers of the Alu-St WP aluminium (2X 1mm thick aluminium), the results showed a significant difference. The polystyrene foam appears to remove part of the fragment energy, limiting its capability to perforate the next plate. Removing the polystyrene foam is not an option because it is there to hold the four aluminium sheets together in the WP and to provide rigidity to the aluminium sheets.

Even if the Alu-St witness pack showed more sensibility to record debris than the All-St WP and is recommended for this type of threat, the PID and PIA calculated with Kokinakis showed closer results than expected. One reason for this is that the Kokinakis model considered some of the lower energy fragments (16 % of the fragments were rejected from the Alu-St WP versus 2 % from the All-St WP) as non-lethal because their energy is beyond the range of validity in the model. It is recommended to redo the analysis using the Computer Man model because this model could be valid for some of those low energy fragments. If so, the difference in sensitivity between the two WP would probably be increased. It seems clear, however, that the Alu-St WP is more sensitive to BAD than the All-St WP.

List of symbols/abbreviations/acronyms/initialisms

All-St	All-Steel
Alu-St	Aluminium-Steel
BAD	Behind-Armour Debris
BISO	Build in Standoff
DeCaM	Debris Characterisation and Modelling software
DRDC	Defence Research and Development Canada
PI	Percentage of Incapacitation
PIA	Percentage of Incapacitation Attack-5 min
PID	Percentage of Incapacitation Defence-30 sec
RHA	Rolled Homogenous Armour
SC	Shaped Charge
TTCP	The Technical Cooperation Program
WP	Witness Pack
WPAS	Witness Pack Analysis System

This page intentionally left blank.

DOCUMENT CONTROL DATA		
(Security markings for the title, abstract and indexing annotation must be entered when the document is Classified or Designated)		
1. ORIGINATOR (The name and address of the organization preparing the document. Organizations for whom the document was prepared, e.g., Centre sponsoring a contractor's report, or tasking agency, are entered in Section 8.) DRDC – Valcartier Research Centre Defence Research and Development Canada 2459 route de la Bravoure Quebec (Quebec) G3J 1X5 Canada	2a. SECURITY MARKING (Overall security marking of the document including special supplemental markings if applicable.) UNCLASSIFIED	2b. CONTROLLED GOODS (NON-CONTROLLED GOODS) DMC A REVIEW: GCEC APRIL 2011
3. TITLE (The complete document title as indicated on the title page. Its classification should be indicated by the appropriate abbreviation (S, C or U) in parentheses after the title.) Comparative incapacitation study between aluminium-steel and all-steel witness packs used to record behind-armour debris from a shaped charge impact		
4. AUTHORS (last name, followed by initials – ranks, titles, etc., not to be used) Baillargeon Y.; Lacoursière P.; Sirois A.		
5. DATE OF PUBLICATION (Month and year of publication of document.) December 2014	6a. NO. OF PAGES (Total containing information, including Annexes, Appendices, etc.) 28	6b. NO. OF REFS (Total cited in document.) 0
7. DESCRIPTIVE NOTES (The category of the document, e.g., technical report, technical note or memorandum. If appropriate, enter the type of report, e.g., interim, progress, summary, annual or final. Give the inclusive dates when a specific reporting period is covered.) Scientific Report		
8. SPONSORING ACTIVITY (The name of the department project office or laboratory sponsoring the research and development – include address.) DRDC – Valcartier Research Centre Defence Research and Development Canada 2459 route de la Bravoure Quebec (Quebec) G3J 1X5 Canada		
9a. PROJECT OR GRANT NO. (If appropriate, the applicable research and development project or grant number under which the document was written. Please specify whether project or grant.)	9b. CONTRACT NO. (If appropriate, the applicable number under which the document was written.)	
10a. ORIGINATOR'S DOCUMENT NUMBER (The official document number by which the document is identified by the originating activity. This number must be unique to this document.) DRDC-RDDC-2014-R147	10b. OTHER DOCUMENT NO(s). (Any other numbers which may be assigned this document either by the originator or by the sponsor.)	
11. DOCUMENT AVAILABILITY (Any limitations on further dissemination of the document, other than those imposed by security classification.) Unlimited		
12. DOCUMENT ANNOUNCEMENT (Any limitation to the bibliographic announcement of this document. This will normally correspond to the Document Availability (11). However, where further distribution (beyond the audience specified in (11) is possible, a wider announcement audience may be selected.) Unlimited		

13. **ABSTRACT** (A brief and factual summary of the document. It may also appear elsewhere in the body of the document itself. It is highly desirable that the abstract of classified documents be unclassified. Each paragraph of the abstract shall begin with an indication of the security classification of the information in the paragraph (unless the document itself is unclassified) represented as (S), (C), (R), or (U). It is not necessary to include here abstracts in both official languages unless the text is bilingual.)

Two witness pack configurations are widely used by The Technical Cooperation Program (TTCP) members to record behind armour debris: the all-steel pack and an aluminium-steel pack. Ballistic impacts were performed for a given shaped charge threat against a specific target to analyse the difference in the behind-armour debris measured using the two different witness packs. This report showed a higher number of fragments recorded and a higher level of incapacitation measured using the aluminium-steel witness pack. The first witness pack layers of the aluminium-steel witness pack are more easily perforated by fragments since they are made of 1 mm of aluminium compared to 0.8 mm of steel for the all-steel pack. Based on this report, it is recommended continuing using the aluminium-steel witness pack for behind-armour debris measurement of a shaped charge impact on a metallic target.

Deux panneaux témoins sont grandement utilisés par les membres du programme de coopération technique (TTCP) pour consigner les débris derrière le blindage : le panneau tout acier et celui en acier à l'aluminium. Des tests d'impact balistique ont été réalisés avec une charge creuse donnée sur une cible déterminée pour analyser la différence de mesure des débris derrière le blindage à l'aide des deux panneaux témoins. Les résultats du présent rapport démontrent qu'un plus grand nombre de fragments a été constaté et qu'un niveau plus élevé d'incapacité a été mesuré à l'aide du panneau témoin en acier à l'aluminium. Les premières couches du panneau témoin en acier à l'aluminium sont plus facilement perforées par les fragments, car elles sont constituées de 1 mm d'aluminium comparativement à 0,8 mm dans le cas du panneau tout acier. En se basant sur le présent rapport, on recommande de continuer à utiliser le panneau témoin en acier à l'aluminium pour mesurer les débris derrière le blindage à la suite de l'impact d'une charge creuse sur une cible métallique.

14. **KEYWORDS, DESCRIPTORS or IDENTIFIERS** (Technically meaningful terms or short phrases that characterize a document and could be helpful in cataloguing the document. They should be selected so that no security classification is required. Identifiers, such as equipment model designation, trade name, military project code name, geographic location may also be included. If possible keywords should be selected from a published thesaurus, e.g., Thesaurus of Engineering and Scientific Terms (TEST) and that thesaurus identified. If it is not possible to select indexing terms which are Unclassified, the classification of each should be indicated as with the title.)

Kokinakis, Shaped charge impact, Witness packs, Behind armour debris, Decam